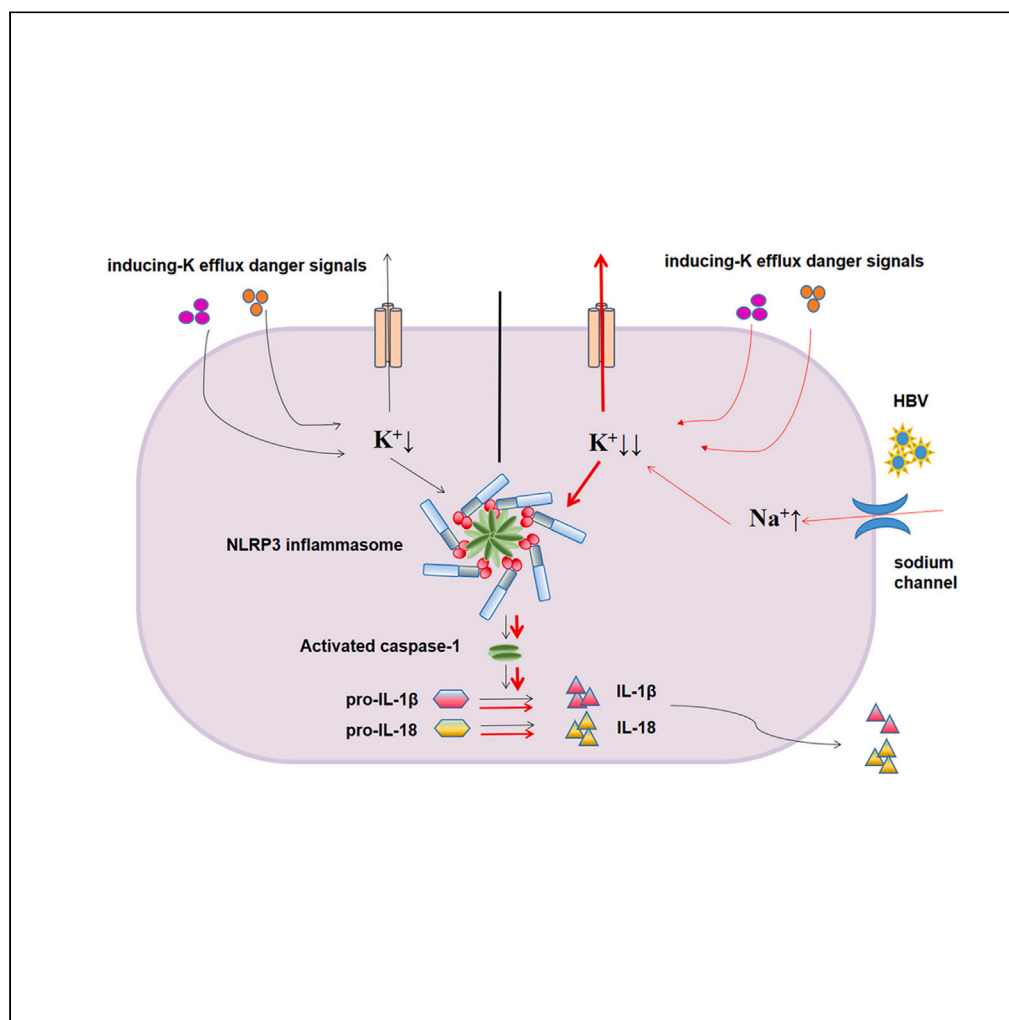


## Article

## Hepatitis B virus-mediated sodium influx contributes to hepatic inflammation via synergism with intrahepatic danger signals



Jingxue Wang,  
Qian Liu, Yiwen  
Zhou, ..., Xiaojuan  
Xin, Guangyu  
Huang, Yuzhang  
Wu

jingxue.wang@hotmail.com  
(J.W.)  
202160@hospital.cqmu.edu.cn  
(X.X.)  
hgy1979@zju.edu.cn (G.H.)  
wuyuzhang@iicq.vip (Y.W.)

**Highlights**

HBV synergism with  
potassium efflux-  
dependent activation of  
NLRP3 inflammasome

HBV cannot activate  
NLRP3 inflammasome  
unless intrahepatic danger  
signals

The NLRP3 inflammasome  
effector cytokines are  
associated with hepatic  
inflammation

HBV promotes sodium  
influx and enhances  
activation of NLRP3  
inflammasome

Wang et al., iScience 27,  
108723  
January 19, 2024 © 2023 The  
Author(s).  
[https://doi.org/10.1016/  
j.isci.2023.108723](https://doi.org/10.1016/j.isci.2023.108723)

## Article

## Hepatitis B virus-mediated sodium influx contributes to hepatic inflammation via synergism with intrahepatic danger signals

Jingxue Wang,<sup>1,8,\*</sup> Qian Liu,<sup>2</sup> Yiwen Zhou,<sup>1</sup> Chunhao Cao,<sup>3</sup> Penghui Chen,<sup>4</sup> Gang Meng,<sup>5</sup> Ji Zhang,<sup>1</sup> Xiaojuan Xin,<sup>6,\*</sup> Guangyu Huang,<sup>7,\*</sup> and Yuzhang Wu<sup>1,\*</sup>

## SUMMARY

**The NACHT, LRR, and PYD domains-containing protein 3 (NLRP3) inflammasome has been involved in the pathogenesis of various chronic liver diseases. However, its role in hepatitis B virus (HBV)-associated hepatitis remains unknown. Here we demonstrate the synergistic effect of HBV with potential intrahepatic danger signals on NLRP3 inflammasome activation. HBV exposure at the appropriate temporal points enhances potassium efflux-dependent NLRP3 inflammasome activation in macrophages and also increases NLRP3 inflammasome-mediated inflammation in HBV-transgenic mouse model. HBV-mediated synergism with intrahepatic signals represented by ATP molecules on NLRP3 activation was observed via relevance analysis, confocal microscopy, and co-immunoprecipitation, and its effector cytokines exhibit positive associations with hepatic inflammation in patients with severe hepatitis B. Furthermore, the synergism of HBV on NLRP3 inflammasome activation owes to increased sodium influx into macrophages. Our data demonstrate that HBV contributes to hepatic inflammation via sodium influx-dependent synergistic activation of NLRP3 inflammasome, which provides a deeper understanding of immune pathogenesis in HBV-associated hepatitis.**

## INTRODUCTION

The host inflammatory response is a critical determinant for occurrence of chronic hepatitis B and its progression to liver cirrhosis and hepatocellular carcinoma. NACHT, LRR, and PYD domains-containing protein 3 (NLRP3) inflammasome has been reported to participate in the pathogenesis of various chronic liver diseases.<sup>1</sup> However, whether NLRP3 inflammasome contributes to hepatitis B virus (HBV)-associated hepatitis remains unclear.<sup>2</sup>

Canonical inflammasomes are multiprotein complexes that assemble to activate caspase-1 in response to danger signals and play a critical role in inflammatory response. Activated caspase-1, represented by p20 subunits, cleaves pro-interleukin (IL)-1 $\beta$ , pro-IL-18, and gasdermin D (GSDMD), which are major inflammasome effectors.<sup>3</sup> NLRP3 inflammasome has been reported to be involved in hepatic inflammation and injury in alcoholic liver disease, nonalcoholic fatty liver disease,<sup>1</sup> hepatitis C,<sup>4</sup> and hepatitis E.<sup>5</sup> Signals derived from gut microbiota, metabolism disorder, and hepatocyte death probably activate NLRP3 inflammasome by potassium efflux, reactive oxygen species (ROS) production, and lysosomal leakage.<sup>6</sup> To date, three pathways have been reported for NLRP3 inflammasome-mediated hepatic inflammation: IL-1 $\beta$ -mediated intrahepatic inflammation,<sup>4</sup> IL-18-induced cytotoxicity,<sup>7</sup> and GSDMD-mediated hepatocyte pyroptosis.<sup>8</sup> The regulatory effect of NLRP3 inflammasome by HBV is not always consistent. Although persisting exposure to HBV inhibits ROS-dependent activation of NLRP3 inflammasome<sup>9</sup> and production of IL-1 $\beta$  in non-CD68<sup>+</sup> macrophages,<sup>10</sup> NLRP3 inflammasome still appears to be involved in the pathogenesis of HBV-associated hepatic failure,<sup>11</sup> and intrahepatic mRNA level of IL-1 $\beta$  also significantly correlates with the level of alanine transaminase (ALT) in patients with a new diagnosis of chronic hepatitis B.<sup>12</sup> Thus, activation and effect of NLRP3 inflammasome in HBV-containing context need to be defined further.

It has been extensively agreed that HBV-mediated immunopathology is mostly caused by bystander activation of killer cells,<sup>2,13–15</sup> especially bystander CD8<sup>+</sup> T cells.<sup>14,15</sup> However, some old questions still need to be answered. For example, what innate pathway in HBV infection is involved in infiltration and bystander activation of CD8<sup>+</sup> T cells? It has been reported circulating intrahepatic antigen-specific CD8<sup>+</sup> T cells

<sup>1</sup>Department of Immunology, Army Medical University, Chongqing, P.R. China

<sup>2</sup>Department of Clinical Laboratory Medicine, Southwest Hospital, Army Medical University, Chongqing, P.R. China

<sup>3</sup>Department of Integrated Traditional Chinese and Western Medicine, The First Affiliated Hospital of Chongqing Medical University, Chongqing, P.R. China

<sup>4</sup>Department of Neurobiology, Army Medical University, Chongqing, P.R. China

<sup>5</sup>Department of Pathology, Southwest Hospital, Army Medical University, Chongqing, P.R. China

<sup>6</sup>Department of Infectious Diseases, The First Affiliated Hospital of Chongqing Medical University, Chongqing, P.R. China

<sup>7</sup>Department of Infectious Diseases, The Fourth Affiliated Hospital Zhejiang University School of Medicine, Yiwu, Zhejiang, P.R. China

<sup>8</sup>Lead contact

\*Correspondence: [jingxue.wang@hotmail.com](mailto:jingxue.wang@hotmail.com) (J.W.), [202160@hospital.cqmu.edu.cn](mailto:202160@hospital.cqmu.edu.cn) (X.X.), [hgy1979@zju.edu.cn](mailto:hgy1979@zju.edu.cn) (G.H.), [wuyuzhang@iicq.vip](mailto:wuyuzhang@iicq.vip) (Y.W.)

<https://doi.org/10.1016/j.isci.2023.108723>



do not infiltrate into the liver<sup>16</sup> unless activation of Toll-like receptor (TLR)/IL-1R signaling pathway recruits them into the liver,<sup>16,17</sup> and bystander activation of killer cell needs IL-18 and some other cytokines.<sup>18</sup> Whether effector cytokines of NLRP3 inflammasome participates in HBV-associated T cell inflammation remains unclear. Some danger signals, such as bacterial infection,<sup>19</sup> uric acid,<sup>20</sup> and high mobility group box 1 (HMGB1), and some drugs, for example anti-tuberculosis drug,<sup>21</sup> exacerbate HBV-related inflammatory response and injury. The mechanism through which inflammatory damage is exacerbated due to crosstalk between these pathogen-associated and damage-associated molecular patterns (PAMPs and DAMPs, respectively) and HBV still remains unknown.

In the present study, we defined synergistic effect of HBV on potassium efflux-dependent NLRP3 inflammasome activation in macrophages and *in vivo* and then verified NLRP3 inflammasome activated by HBV-mediated synergism was involved in onset of HBV-related hepatic inflammation in patients. Furthermore, we investigated the synergistic mechanism by which enhanced activation of NLRP3 inflammasome was induced by HBV in macrophages.

## RESULTS

### HBV displays a synergistic effect on potassium efflux-dependent NLRP3 inflammasome activation in macrophages

To define the effect of HBV on NLRP3 inflammasome, we investigated NLRP3 inflammasome activation triggered by different signals in the context of HBV. As shown in Figure 1A, we observed nigericin, which was a microbial toxin that activates NLRP3 inflammasome via triggering K<sup>+</sup> efflux, in combination with HBV, enhanced NLRP3 inflammasome activation and increased cleavage and secretion of IL-1 $\beta$  and caspase-1 p20 subunit in murine bone marrow-derived macrophages (BMDMs). The monosodium urate monohydrate (MSU) signal, another trigger for potassium efflux<sup>22</sup>-dependent NLRP3 activation via sodium overloading,<sup>23</sup> in combination with HBV, also enhanced cleavage and release of IL-1 $\beta$  in BMDMs (Figures 1B and S1A). A similar HBV-mediated enhancement on MSU-induced NLRP3 activation was observed in the human peripheral blood mononuclear cells (PBMCs, Figure 1C) and THP-1-derived macrophages (Figure S1B). In iniquimod-triggered NLRP3 activation, which is ROS-dependent but not K<sup>+</sup> efflux-dependent activation, HBV did not increase the cleavage of IL-1 $\beta$  and caspase-1 p20 (Figure 1D). HBV also reduced poly(dA:dT)-induced AIM2 inflammasome activation (Figure S1C). Raising extracellular K concentration gradually to 40 mM with 2 M KCl solution would inhibit NLRP3 activation by canonical and non-canonical activators<sup>24</sup> with different extents. HBV made activation of NLRP3 inflammasome more resistant to extracellular high potassium, but not ROS scavenger N-acetyl cysteine (NAC), which implies HBV enhances NLRP3 inflammasome via enhancement of potassium efflux signals rather than ROS signals (Figures 1A, 1B, and S1D). The HBV-mediated enhancement did not display a clear linear association with HBV dose (Figure S1E), which implied that the synergistic effect was mediated by interaction between viral protein and certain cellular membrane receptor and presented a saturation effect due to limited expression of cellular membrane receptor. HBV alone, or in combination with lipopolysaccharide (LPS) treatment, cannot activate NLRP3 inflammasome in macrophages (Figures 1D and S1A), which suggests HBV cannot trigger directly potassium efflux without simultaneous potassium efflux-inducing signals and only synergize with these signals to enhance potassium efflux. HBV-mediated enhancing effect was expanded after 24 h of HBV exposure and subsequent 24 h of rest (Figure 1E), although the transcription and activation of NLRP3 inflammasome reduced in macrophages upon persistent exposure to HBV for 17 h without withdraw (Figures S1F and S1G). To exclude indirect effect derived from ATP release probably induced by HBV exposure in macrophages, we investigate whether the synergism would be blocked by P2X7 inhibitors, A438079, A740003, and suramin. Our data show blockage of ATP/P2X7 pathway does not prevent HBV-mediated synergistic effects (Figures 1A and 1F). And L47, a synthesized PreS1(2–47), also displays such synergistic effect with nigericin (Figure 1E). Our data suggest that HBV displays a synergistic effect with danger signals on K efflux-dependent but not ROS-dependent NLRP3 activation through interaction between viral surface protein and macrophages.

### HBV exacerbates inflammatory response *in vivo* through synergistic effect on NLRP3 inflammasome

We further induced peritonitis model with MSU, a classical NLRP3 inflammasome mouse model,<sup>25</sup> in HBV-transgenic (tg) mice (n  $\geq$  8) and wild-type mice to investigate whether HBV can enhance NLRP3 inflammasome-dependent inflammatory infiltration *in vivo*. We observed increased NLRP3 inflammasome-dependent neutrophil infiltration and IL-1 $\beta$  release in the abdominal cavity of HBV-tg mice (Figures 2A–2C) compared to wild-type mice, which suggested that HBV enhanced the activation of NLRP3 inflammasome *in vivo* and led to more robust inflammatory infiltration. Because the nucleoside analogue can directly inhibit NLRP3 inflammasome,<sup>26</sup> we did not use entecavir treatment as a negative control in the aforementioned HBV-tg mouse experiments.

To investigate inflammatory response in patients, we selected a group of patients with cirrhosis and primary peritonitis (as shown in the Table 1) and compared inflammatory response between HBV-infected and non-HBV-infected cirrhosis. We observed that HBV infection led to higher C-reactive protein (CRP) level, a downstream response factor of inflammasome<sup>27</sup> and a biomarker for inflammation,<sup>28</sup> in patients with HBV-associated cirrhosis and primary peritonitis (Figure 2D), which implied that HBV also promotes inflammatory response in patients.

### NLRP3 inflammasome is activated by HBV-mediated synergism with intrahepatic danger signals in patients with severe hepatitis B

To investigate inflammasome status in patients with chronic HBV infection, we selected two groups of patients: outpatients with HBV infection with minimal hepatic inflammation and inpatients with HBV-associated active severe hepatitis. In active severe hepatitis group (defined as modified histological activity index [HAI]  $\geq$  6, or either of the following three conditions: an abrupt elevation in serum ALT  $\geq$  200 IU/mL, total

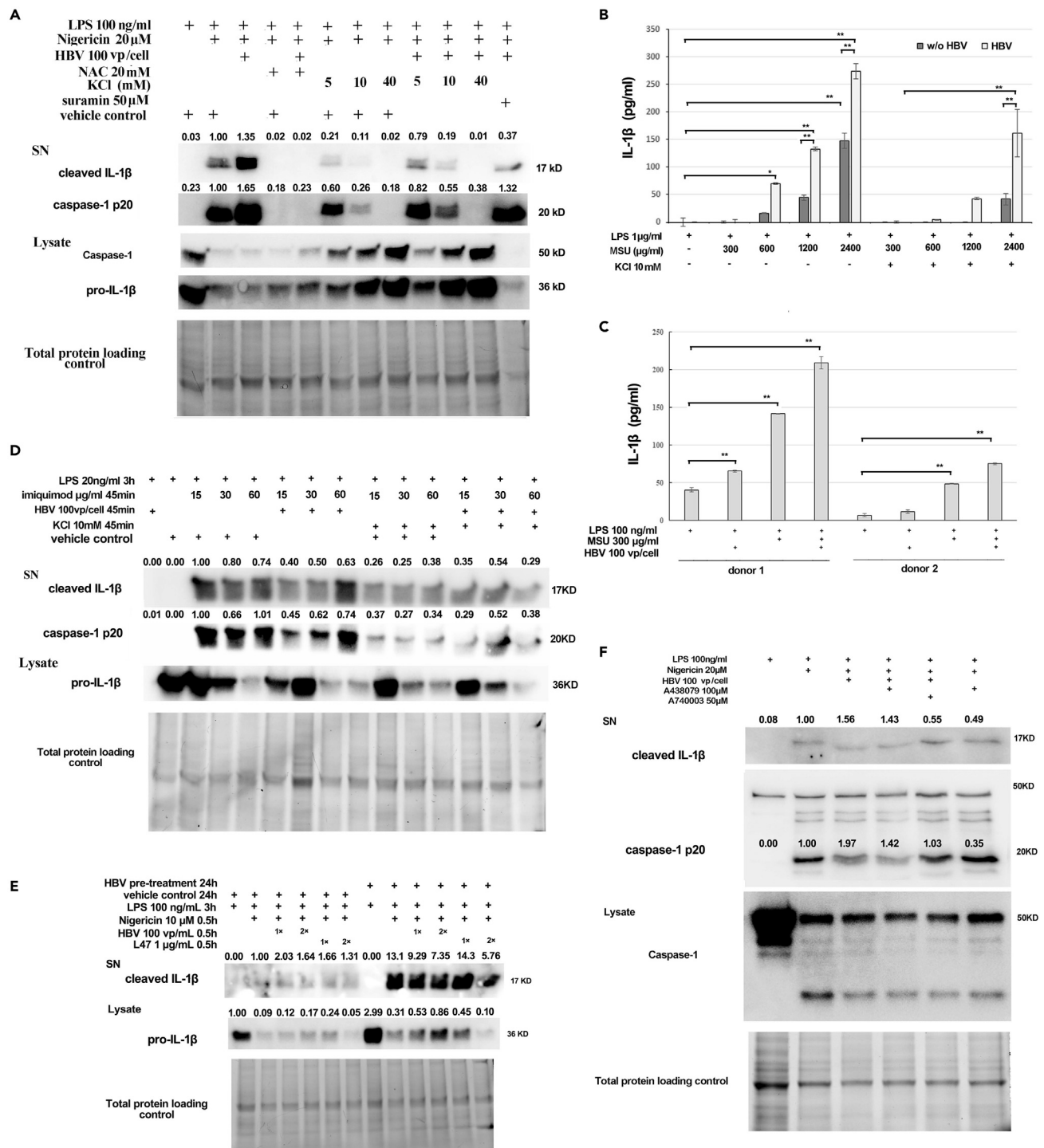


**Figure 1. HBV promotes potassium efflux-dependent NLRP3 inflammasome activation in macrophages**

LPS was added for 3 h before stimulation with nigericin for 0.5 h in the BMDMs (A, F), MSU for 6 h in the BMDMs (B) and PBMCs derived from healthy donors (C) and imiquimod for 45 min in the BMDMs (D). The potassium chloride was used to raise the extracellular potassium concentration in order to block intracellular potassium efflux.

(E) The BMDMs upon HBV pre-treatment for 24 h and then rest for 24 h were stimulated with LPS and nigericin combined with HBV particles or L47 peptides. The supernatant (SN) or cell extracts (Lysate) were analyzed by western blotting (WB) or ELISA, as indicated. The quantitative measurement of WB data was performed using Image Lab software normalized to total protein loading control. Data, except for the C group, are representative of five independent experiments;  $p < 0.05$  was considered significant; \* $p < 0.05$  and \*\* $p < 0.01$ . Abbreviations: vp, viral particles.

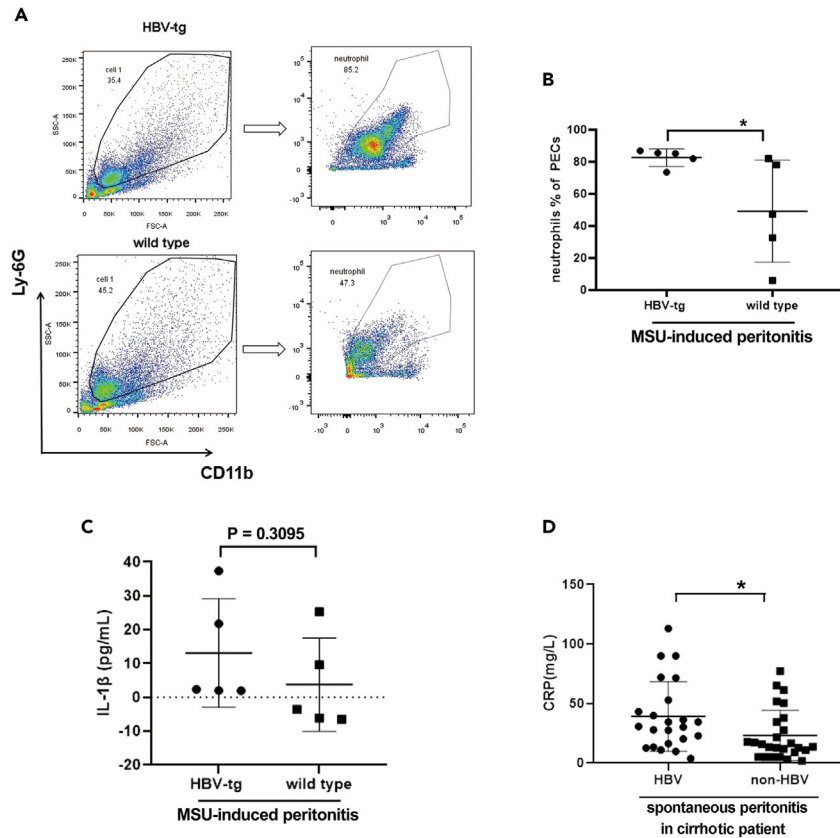


**Figure 2. HBV exposure enhances immune cell infiltration and inflammatory response in vivo**

MSU crystal-induced peritonitis HBV-tg or wild-type mouse model were used to assess effect of HBV exposure on inflammatory response in vivo. The MSU in PBS (150  $\mu$ L, 5 mg/mL) was injected into the peritoneal cavity of mouse, and cells in the intraperitoneal lavage fluid were harvested upon 6 h and assayed using flow cytometry. Representative figures of Ly6G<sup>+</sup>CD11b<sup>+</sup> neutrophil(A) and data for 5 mice in each group(B) are shown. The interleukin-1 $\beta$  in the lavage fluid were assayed using ELISA and data for 5 mice in each group(C) are shown.

(D) The CRP levels were compared between HBV-infected and non-HBV-infected patients with cirrhosis with primary peritonitis. PECs, peritoneal exudate cells. All data were analyzed using the GraphPad Prism 8.0 software.  $p < 0.05$  was considered significant; \* $p < 0.05$  and \*\* $p < 0.01$ .

bilirubin (TBIL)  $\geq 100 \mu$ M, and international normalized ratio [INR]  $\geq 1.2$ <sup>29–31</sup> as shown in Table 2), we observed increased caspase-1 p20, IL-1 $\beta$ , and IL-18 levels in the plasma compared with healthy controls (Figures 3A–3C). In the group with minimal hepatitis (defined as modified HAI  $< 6$ , ALT  $< 40$  IU/mL, and TBIL  $< 25 \mu$ M, as shown in first and third row of Table 3), these markers in the plasma were not increased compared to those in healthy controls (Figures 3E and 3F) except for IL-18 (Figure 3G). We also assayed some patients with chronic moderate hepatitis B (40 IU/mL  $<$  ALT  $< 200$  IU/mL,  $25 \mu$ M  $<$  TBIL  $< 100 \mu$ M, and INR  $< 1.2$ , as shown in second and fourth row of Table 3) and observed IL-18 to be similarly increased in the plasma (Figure S2A). To confirm intrahepatic activation of inflammasomes, we assayed caspase-1 activity in some HBV-infected liver tissues derived from the fourth-group patients (The HAI score for each patient was shown in Table 4); we observed an increase of intrahepatic caspase-1 activity in these patients (Figure 3D). Notably, there were two patients (No. 1 eAg<sup>+</sup> and No. 9 eAg<sup>-</sup>) with minimal inflammation and normal ALT level but high caspase-1 activity (optical density [OD] value: 0.261, 0.222). These data suggest that intrahepatic inflammasome is activated in patients with HBV-associated active severe hepatitis, and also probably in HBV-associated minimal hepatitis, although only IL-18 among biomarkers of inflammasome activation in the plasma is increased.

**Table 1. Clinical characteristics of patients of first group with cirrhosis and primary peritonitis**

Patients	Sex; Age	HBV infection	INR	Na (mM)	C-reactive protein (mg/L)	Figure
23	m 19; f 4 28–72	positive	1.44 $\pm$ 0.32	137.96 $\pm$ 4.53	39.36 $\pm$ 28.6	Figure 2E; Figures 7A and 7B
26	m 20; f 6 27–82	negative	1.35 $\pm$ 0.22	139.54 $\pm$ 3.13	23.31 $\pm$ 20.84	Figure 2E; Figure S5A

**Table 2. Clinical characteristics of patients of second group with active severe hepatitis B**

Patients	Sex; Age	HBV DNA (IU/mL)	ALT (IU/mL)	INR	TBIL ( $\mu$ M)	Figure
33	m 25; f 8 24–56	0–7.8 $\times$ 10 <sup>8</sup>	42–2222	0.89–2.7	6.2–596.1	Figures 3A–3C, 5A, and 5B

To confirm that NLRP3 inflammasome participates in activation of aforementioned inflammasome, we investigated activation and assembly of NLRP3 inflammasome in liver tissues with HBV-associated active severe hepatitis and observed a clear colocalization of NLRP3 and caspase-1 within intrahepatic infiltrated immune cells (Patient No. 14 in Table 4, HAI score = 13) and hepatocytes (Patient No. 15 in Table 4, HAI score = 8). In the two patients, the CD68<sup>+</sup> intrahepatic macrophages were increased, and major intrahepatic cells produced cleaved IL-1 $\beta$  (17KD [kilodaltons]), as shown in Figures 6E and 6C. Both production of caspase-1 p10 subunits and assembly of NLRP3 inflammasome were increased in the liver tissue from other patients with active severe hepatitis B through western blotting (WB) and co-immunoprecipitation (Figures 4B and 4C), although the expression of NLRP3 was not increased (Figure S2B). Convincing colocalization of NLRP3 inflammasome components was not observed in the liver tissues from healthy control (Figure 4A). In patient no. 15, assembly of NLRP3 inflammasome in the hepatocytes seems not to result in cleavage of IL-1 $\beta$  by caspase-1, because the signals recognized by anti-cleaved IL-1 $\beta$  were majorly in CD68<sup>+</sup> macrophages and not hepatocytes (Figure S2C). Although we did not observe colocalization of NLRP3 and caspase-1 in patient no. 17 (HBV-associated minimal hepatitis), the caspase-1 was displayed like a speck in some hepatocytes and CD68<sup>+</sup> macrophages, and cleaved IL-1 $\beta$  was predominantly located in CD68<sup>+</sup> macrophages, whereas IL-18 can be expressed by hepatocytes (Figure S2D). To assay inflammasome function in the hepatocytes, we applied an *in vitro* HepG2-NTCP model. We observed the release of caspase-1 p20 subunits and 18KD IL-18, but not 17KD IL-1 $\beta$ , in the medium upon HBV infection after 48 h, although 36KD pro-IL-1 $\beta$  can be assayed in the lysate and supernatant of HepG2-NTCP cell lines (Figure S2E), which suggested inflammasome in hepatocytes could succeed to be activated but not effectively cleave pro-IL-1 $\beta$ . Lastly, we performed transcriptome analysis of liver tissue with HBV-related minimal and active severe inflammation. The inflammasome-associated components displayed an increasing expression trend with the extent of hepatic inflammation (Figure 4D), and gene ontology (GO) enrichment analysis of the differentially expressed proteins between minimal and severe hepatic inflammation show that Nod-like receptor signaling pathway was enriched (Figure 4E). Our data suggest that NLRP3 inflammasome might be frequently activated in hepatocytes and intrahepatic CD68<sup>+</sup> macrophages of patients with severe or minimal HBV-associated hepatitis, but production of downstream effectors, especially mature IL-1 $\beta$ , probably is largely from CD68<sup>+</sup> macrophages. Due to inefficiency of hepatocytes in mature IL-1 $\beta$  production, activation of intrahepatic inflammasome is difficult to be verified by plasma samples, unless substantial activation appears within intrahepatic CD68<sup>+</sup> macrophages.

To identify the signals to be responsible for activation of NLRP3 inflammasome, we further analyzed the association between potential triggers and caspase-1 p20 subunits in patients with HBV-associated active severe hepatitis. The levels of caspase-1 p20 subunits show a positive association with ATP levels and HBV DNA copies in the plasma (Figures 5A and 5B), whereas the other signals did not show similar trends (Figure S3A). In healthy controls, the level of caspase-1 p20 subunits did not show a significant positive association with ATP level (Figure S3B).

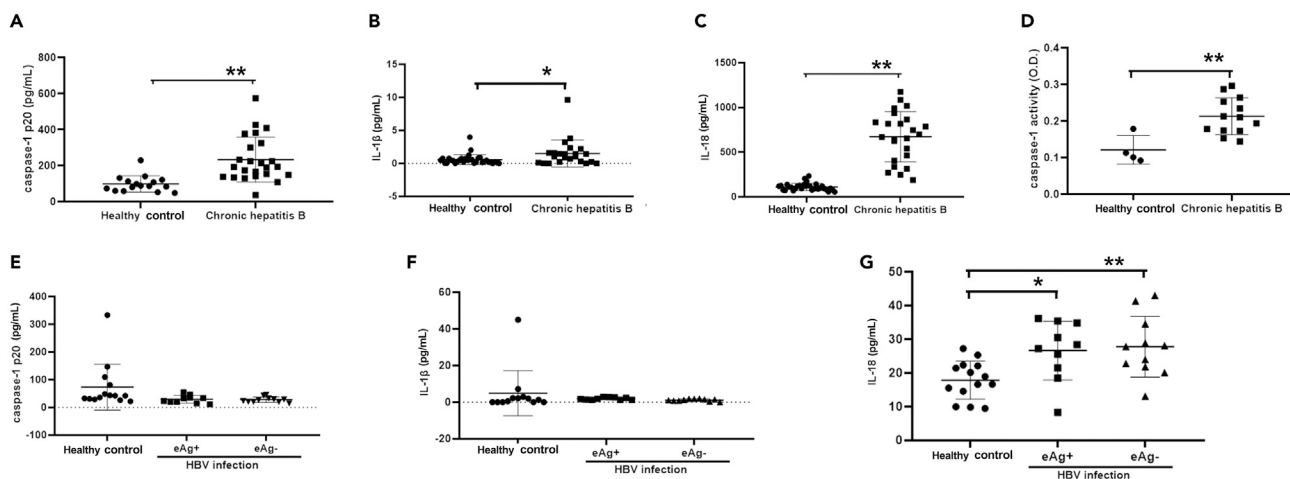


**Figure 3. The periphery markers and intrahepatic inflammasome activity were increased in patients with active severe hepatitis B**

(A) Caspase-1 p20 subunits, (B) IL-1 $\beta$ , and (C) IL-18 in plasma derived from patients with active severe CHB and healthy donors were assayed using ELISA. (D) Liver tissue lysates (100  $\mu$ g) from patients with HBV infection and healthy donors were assayed for caspase-1 activity. In plasma derived from patients with HBV infection without active hepatic inflammation, caspase-1 p20 subunits (E), IL-1 $\beta$  (F), and IL-18(G) were assayed using ELISA. Each dot represents an individual patient.  $p < 0.05$  was considered significant; \* $p < 0.05$  and \*\* $p < 0.01$ .

**Table 3. Clinical characteristics of patients of third group with minimal hepatitis B**

Patients	Sex; Age	HBV DNA (IU/mL)	ALT (IU/mL)	TBIL ( $\mu$ M)	HBeAg	INR	Figure
10	f 6; m 4 33.8 $\pm$ 8.3	2-2340 $\times$ 10 <sup>5</sup>	24.7 $\pm$ 7.9	11.7 $\pm$ 4.5	positive	<1.2	Figures 3E–3G
7	f 5; m 2 23.8–62	0.5–3860 $\times$ 10 <sup>5</sup>	41–89	2.3–37.6	positive	<1.2	Figure S2A
11	f 6; m5; 42.3 $\pm$ 12.6	<1.96 $\times$ 10 <sup>3</sup>	25 $\pm$ 9.9	10.9 $\pm$ 3.6	negative	<1.2	Figures 3E–3G
18	f 7; m11; 25–66	0-28 $\times$ 10 <sup>5</sup>	42–147	7.3–74.7	negative	<1.2	Figure S2A

Using an *in vitro* ATP stimulation in macrophages, we observed ATP-triggered NLRP3 inflammasome activation was enhanced in phorbol 12-myristate 13-acetate (PMA)-treated THP-1 cells (Figure 5C) and mouse BMDMs upon HBV exposure (Figure 5D). HBV alone did not activate NLRP3 inflammasome (Figure 5C); however, HBV displayed a synergistic effect on ATP-induced cleavage of IL-1 $\beta$  (Figures 5C and 5D), just as on nigericin and MSU. P2X7, a critical factor for ATP-triggered inflammasome activation, also bound with NLRP3 and caspase-1 molecules in the liver tissue of patient with HBV-associated severe hepatitis (Figures 4A and 4C). Our data suggest that the synergism between HBV and ATP molecules, one of representative intrahepatic danger signals, participates in activation of NLRP3 inflammasome in patients with HBV-associated severe hepatitis.

### The effector cytokines of NLRP3 inflammasome promoted liver injury and inflammation in patients with active severe hepatitis B

In patients with active severe hepatitis B, inflammasome-induced IL-18 shows to be positively associated with liver injury marker, ALT, and M30 serum cytokeratin-18 epitopes (Figures 6A and 6B). And GSDMD-associated hepatocyte death did not seem to be a major contributor to HBV-mediated inflammatory injury, since only a few C-terminal of GSDMD-positive hepatocytes were observed in the liver of patients with minimal or severe hepatitis B, compared to that in HBV-related hepatocellular carcinoma (Figure S4A). Due to intrahepatic production of mature IL-1 $\beta$  majorly by CD68<sup>+</sup> macrophages but not hepatocytes (Figures S2C–S2E; Figures 6C and 6D), we analyzed the number of CD68<sup>+</sup> macrophages in each representative patient with different extents of hepatic inflammation. The numbers of CD68<sup>+</sup> macrophages were gradually increased in hepatic microenvironment with inflammation aggravation (Figures 6E and 6G). Notably, in pooled data of 2 patients with minimal hepatitis from multiplexed immunofluorescence staining, we observed decreased intrahepatic CD68<sup>+</sup> macrophages (Figure 6E) and decreased mature IL-1 $\beta$  but not IL-18 production compared to healthy control (Figures S4B and S4C), similar with the trend of plasma sample data (Figures 3F and 3G). Thus, the unsynchronized generation of IL-1 $\beta$  and IL-18 in HBV-infected liver probably lead to different effects; for example, IL-1 $\beta$  was not positively associated with ALT (Figure S4D). The CD8<sup>+</sup> T cells have been reported to contribute to hepatic inflammation and injury in patients with severe hepatitis. We observed the number of CD8<sup>+</sup> T cells was increased with degree of hepatic inflammation (Figures 6F and 6G) and displayed a positive association with CD68<sup>+</sup> cells (Figure 6H) and IL-1 $\beta$ <sup>+</sup> (Figure 6I) but not IL-18<sup>+</sup> particles (Figure S4E) in random visual fields of liver tissue slides with severe hepatitis B. Because the mature IL-1 $\beta$  is largely produced by intrahepatic CD68<sup>+</sup> cells, but not CD8<sup>+</sup> T, our data imply IL-1 $\beta$  produced by CD68<sup>+</sup> macrophages contributes to intrahepatic accumulation of CD8<sup>+</sup> T cells in patients with severe hepatitis B, via either IL-1R-mediated recruitment<sup>16,17</sup> or proliferation<sup>32</sup> demonstrated by previous reports. These findings suggest that NLRP3 inflammasome activation in severe hepatitis B contributes to hepatic inflammation and damage through IL-18-induced hepatocyte death and IL-1 $\beta$ -mediated CD8<sup>+</sup> T cell accumulation.

### HBV-mediated sodium influx results in synergistic effect on NLRP3 inflammasome in macrophages

By analyzing clinical data from patients with cirrhosis with primary peritonitis, we observed that sodium concentration in the serum of HBV-infected patients was lower than that of non-HBV-infected patients (Figure 7A) and significantly negatively associated with CRP levels (Figure 7B). We did not observe such a significant negative association in 26 patients with non-HBV-related primary peritonitis (Figure S5A). We further observed voltage-gated sodium channels (VGSCs), including Nav1.5, Nav1.6, and Nav1.7 as reported by previous study,<sup>33,34</sup> were expressed in HBV-infected liver; however, only Nav1.5 was found to be distinctly upregulated by HBV infection (Figure S5B). We then examined whether HBV exposure in macrophages interfered with sodium ion traffic. In an artificially high intracellular sodium environment (190 mM sodium), exposure to HBV resulted in an outward current that persisted for almost 100 ms in THP-1 macrophages (Figure S5C). If the intracellular solution was changed to a traditional potassium solution (154 mM potassium), the outward current disappeared. The Current-Voltage curve (IV curve) activated by depolarizing steps from  $-60$  mV to  $+60$  mV (10 mV increment) is a classical assay for VGSC currents in the neuronal system.<sup>35</sup> On applying depolarizing step pulses, we observed the IV curve in THP-1 macrophages exposed to HBV displayed a robust and considerable fluctuation of the IV curve. The non-specific sodium channel blocker diphenylhydantoin sodium (DPH) reduced such fluctuation (Figure S5D). To compare such fluctuations, we

**Table 4. Clinical characteristics of patients of fourth group with chronic HBV infection**

Patient No.	Sex/Age	HBV DNA (IU/mL)	INR	ALT (IU/mL)/TBIL ( $\mu$ M)	HAI score	Fibrosis score	Experiment
1	f/32	18600000	NA	23/NA	3	0	A
2	m/44	8600000	1.77	136/120	15	2	A
3	m/48	4660000	1.34	71/154	12	2	A
4	m/28	53700000	0.91	258/18	7	2	A, WB
5	m/40	12980	1.11	410/55.1	15	5	A
6	m/22	6190	0.86	2436/97	12	2	A
7	m/37	7880	0.8	56/-	5	0	A
8	m/33	2290	1.54	621/222.2	7	2	A
9	m/41	2940	0.87	22/10.1	4	0	A
10	m/37	<100	0.98	398/46.6	13	2	A
11	f/34	41000	0.97	41/8.8	8	3	A, colP
12	m/41	414000	0.85	2400/116	13	2	A
13	m/24	29700000	0.99	44/14.2	7	2	A
14	m/33	15600000	NA	1999/NA	13	3	IH, Confocal
15	f/45	34500000	NA	35/NA	8	0	IH, Confocal
16	m/26	23070000	1.65	2545/267.6	8	2	WB, colP
17	m/34	<100	NA	<40/NA	3	1	IH, Confocal
18	m/25	117000000	NA	78/NA	8	2	IH
19	m/45	8570	NA	140/NA	4	0	IH
20	f/24	<100	1.0	22/13.1	6	6	RS
21	f/37	8240	1.05	26/13.4	4	5	RS
22	m/47	6050000000	1.76	2294/130	12	2	RS
23	m/52	18500000	1.61	399/470	12	2	RS

A: caspase-1 activity assay; colP: co-immunoprecipitation; IH: immunofluorescence histochemistry; RS: RNA sequence; NA: not available.

selected the inward sodium current activated by  $-20$ mV depolarizing pulse as a metric of HBV interference. The sodium current upon HBV exposure was significantly enhanced compared to that without HBV exposure and DPH treatment (Figure 7C). Furthermore, DPH also inhibited the synergistic effect of HBV on MSU- and nigericin-induced NLRP3 activation (Figures 7D and 7E). Thus, these findings suggest that the HBV-mediated synergistic effect results from promotion of influx of sodium ions into macrophages, probably via VGSCs.

## DISCUSSION

The role of NLRP3 inflammasome in HBV-associated chronic liver disease is not well understood, largely due to limited knowledge on how HBV regulates NLRP3 inflammasome. It has been known activation of NLRP3 inflammasome requires priming and activating signals. Our data suggest that HBV enhances activating signals mediated by K efflux via promoting sodium influx into macrophages and reduces activating signal mediated by imiquimod-induced mitochondrial ROS,<sup>36</sup> which implies HBV can regulate NLRP3 activation in multiple levels and be dependent on different activators. Potassium efflux activates NLRP3 inflammasome in different manner from imiquimod, although they both generate ROS. HBV may inhibit imiquimod-induced NLRP3 activation via previously reported p47<sup>phox</sup>-NOX2-mitochondrial ROS pathway,<sup>9</sup> but it still enhances K efflux-induced NLRP3 activation. This enhancement could be inhibited by NAC through more extensive ROS clearance beyond NOX2 pathway,<sup>37</sup> which implies potassium efflux-dependent ROS production could be independent of NOX2. Notably, HBV cannot activate NLRP3 inflammasome in the absence of concomitant activators, which is consistent with the characteristics of stealth virus. In addition, upon persistent exposure to HBV and subsequent rest for 24 h, the priming signal of NLRP3 inflammasome seems to also be increased, although persisting exposure to HBV without withdrawal would reduce the transcription and activation of NLRP3 inflammasome, as previous reports.<sup>9,10</sup> Priming of NLRP3 inflammasome in hepatocytes was reduced upon persisting exposure to HBV for 17 h, but activation still could be enhanced by synergism between ATP and HBV according to the data from liver tissue slides and HepG2-NTCP, which probably results from different epigenetic regulation of inflammasome components between macrophages and hepatocytes by HBV. In summary, our data suggest intrahepatic NLRP3 inflammasome is regulated by HBV at multiple levels in different manners and presents a high heterogeneity in HBV-infected livers, which depends on priming and activating signals, exposure duration to HBV and subsequent rest duration, cellular types, etc.

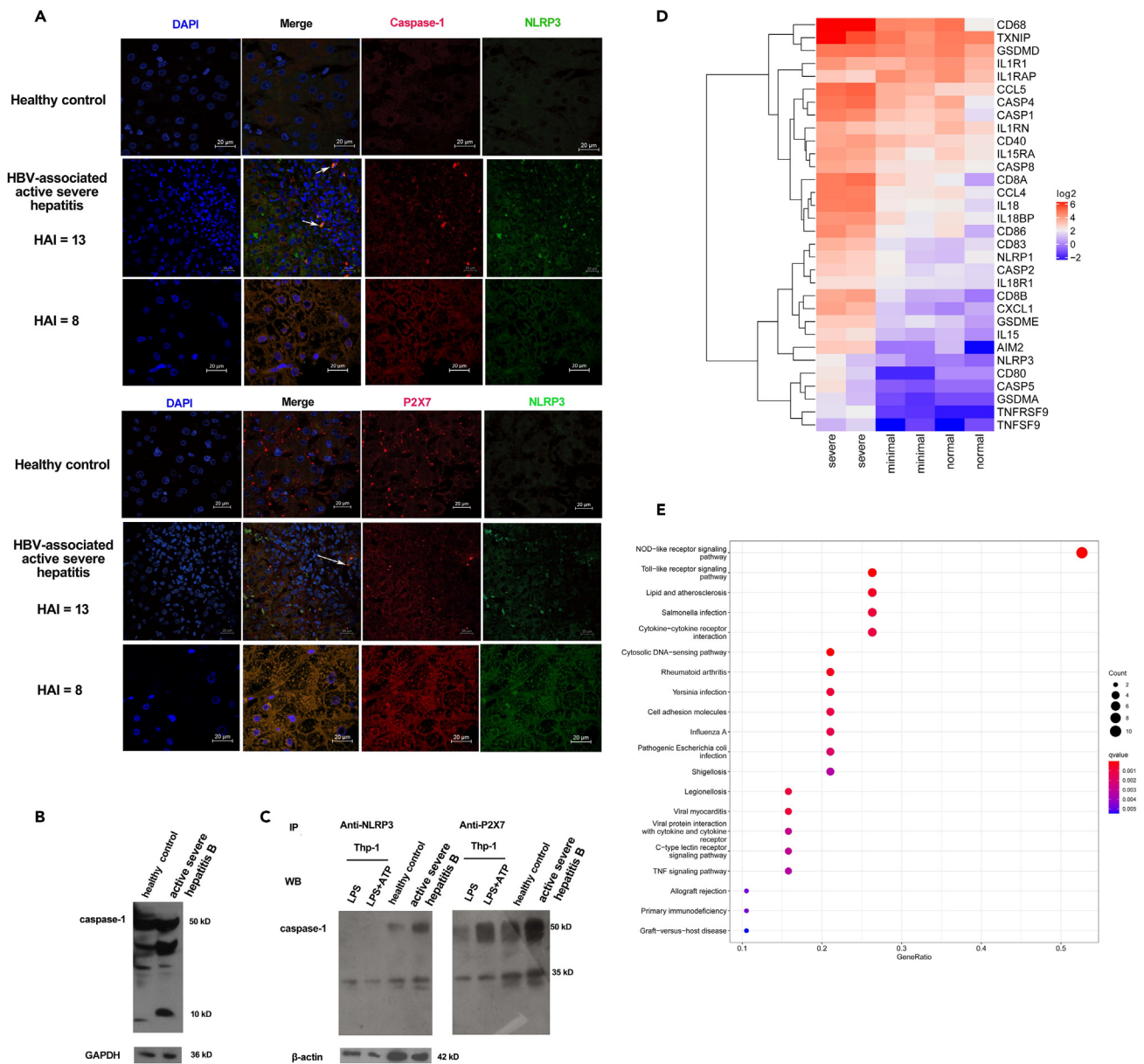


**Figure 4. The intrahepatic activation of NLRP3 inflammasome was enhanced in patients with active severe hepatitis B**

(A) Confocal microscopy figures of liver biopsies from 2 patients with HBV-associated severe hepatitis confirmed the colocalization of caspase-1, NLRP3, and P2X7 in the inflammatory infiltrates (middle panel) and hepatocytes (lower panel) at a resolution of 20 microns.

(B) Western blotting analysis of liver tissue-derived total protein (60  $\mu$ g). Data are representative of two independent experiments.

(C) Liver tissue-derived total protein (100  $\mu$ g) was captured by anti-NLRP3 and anti-P2X7 cross-linked to magnetic beads and assayed by anti-caspase-1 using WB. Data are representative of two independent experiments.

(D) Heatmap of transcriptome data showing differential gene expression in patients with different extents of hepatic inflammation. Each panel indicates an individual with/without HBV infection.

(E) KEGG enrichment analysis of differentially expressed proteins between minimal and severe hepatic inflammation groups. The bubble figure shows the top 20 enriched terms.

The enhancement of K efflux signal by HBV is due to increasing sodium influx into macrophages. Sodium has been reported to be involved in the pathogenesis of autoimmune diseases, certain infectious diseases, angiocardopathy,<sup>38</sup> and chronic liver failure,<sup>39</sup> but effect of sodium on immune response remains ongoing areas of exploration. We reported firstly that HBV exposure resulted in a much greater sodium influx into macrophages and synergize on potassium efflux-triggered NLRP3 activation, which suggests a pathway for sodium to regulate immune response and result in inflammatory injury. Such sodium influx is probably different from

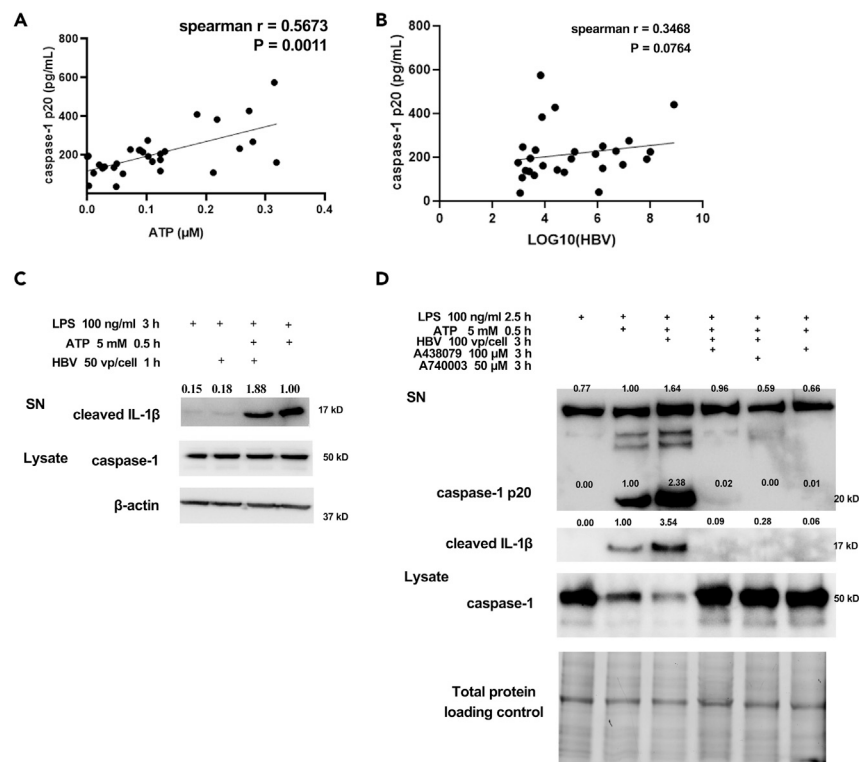


**Figure 5. HBV DNA copies and ATP levels were positively associated with inflammasome activation in patients with active severe hepatitis B**

The linear relationships between ATP levels (A), HBV DNA copies (B), and caspase-1 p20 levels in the plasma of patients with active severe hepatitis B were shown and analyzed by Spearman correlation. ATP molecules, with or without HBV exposure, activated the NLRP3 inflammasome in PMA-treated THP-1 macrophages (C) and BMDMs (D). Cell-free supernatants (SNs) were analyzed for the presence of cleaved IL-1 $\beta$  (17kD) and caspase-1 p20 subunit by WB. Data were representative of three independent experiments. Abbreviations: vp, viral particles.

sodium overload induced by MSU crystal, which can independently trigger NLRP3 activation,<sup>23</sup> but sodium influx mediated by HBV exposure is insufficient for NLRP3 activation. Our data indicated Nav1.5 was upregulated by HBV infection, and the sodium influx mediated by HBV exposure persists over 100 ms, which is also consistent with the characteristic of slow-sodium channel Nav1.5. However, which sodium channel is involved needs to be further defined. Collectively, our data indicate sodium influx enhances potassium efflux-dependent NLRP3 inflammasome activation in macrophages, which also implies a potential mechanistic link between extensive sodium-associated diseases and NLRP3 inflammasome.

The synergism of HBV on NLRP3 inflammasome may play a critical role in provoking inflammatory response of CD68<sup>+</sup> macrophages in HBV-infected liver. Although HBV alone cannot directly activate NLRP3 inflammasomes, the liver is readily enriched for numerous danger signals derived from metabolic dysregulation, endogenous damage, and infection to induce potassium efflux,<sup>1</sup> which probably do not induce a high-grade inflammation in the absence of HBV due to a specific intrahepatic tolerant environment.<sup>40</sup> We indeed observed frequent activation of inflammasome in intrahepatic CD68<sup>+</sup> macrophages of patients with severe or minimal hepatitis B, but limited quantities of intrahepatic CD68<sup>+</sup> macrophages reduce total activating and effect level of NLRP3 inflammasome in patient with minimal hepatitis B. In patients with severe hepatitis B, we observed some proof to verify the synergism. The synergism between HBV and PAMPs/DAMPs also provides a sight into immunological mechanisms by which bacterial infection and metabolic disorder usually exacerbate liver injury in HBV-infected patients.

NLRP3 inflammasome and its effectors have been reported to be the major pathway for triggering hepatic inflammation and injury.<sup>1,40</sup> IL-18, a key bystander signal and effector of NLRP3 inflammasome, is able to activate natural killer (NK) and bystander CD8<sup>+</sup> T cells, which result in hepatocyte death in viral hepatitis.<sup>7,18</sup> Our data indicate IL-18 can be produced by macrophages and hepatocytes in HBV-infected liver and show significant positive associations with hepatocyte death markers in patients with severe hepatitis B, which suggests a mechanistic link between HBV and bystander activation of NK and CD8<sup>+</sup> T cells. And another effector, IL-1 $\beta$ , displays a significant positive association with the number of intrahepatic CD8<sup>+</sup> cells, which implies NLRP3 inflammasome-induced IL-1 $\beta$  contributes to increasing CD8<sup>+</sup> cells response via either recruitment or proliferation.<sup>16,17,32</sup> However, whether IL-1 $\beta$  results in injury could depend on local frequency of HBV-specific CD8<sup>+</sup> T cells, local cytokines milieu, and local amount and function of CD68<sup>+</sup> macrophages. Collectively, we propose an upstream mechanism for HBV-associated T cell inflammation, which might provide a new therapeutic target for improving HBV-specific CD8<sup>+</sup> T cell response.

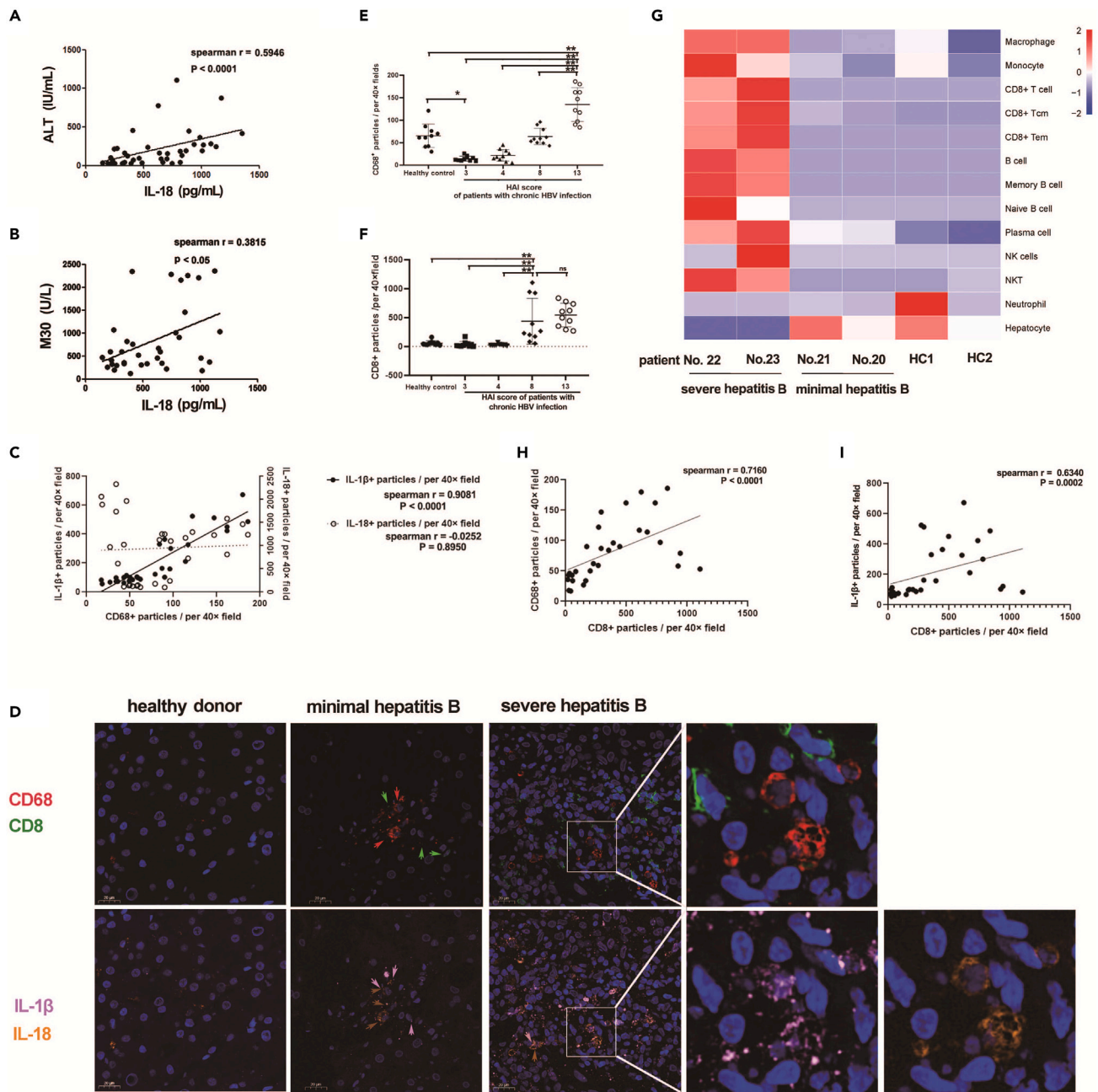


**Figure 6. NLRP3 inflammasome-mediated effector cytokines contributed to liver injury and hepatic inflammation in patients with severe hepatitis B** (A and B) Correlation between IL-18 level and ALT (A) or M30 (B) levels was analyzed in the plasma of inpatients with active severe hepatitis B.

(C–F, H, and I) Liver tissue slides derived from HC and patients with minimal and severe hepatitis B were assayed using TSA-amplified multiplexed immunofluorescence staining. On the same slide, CD68 (red), CD8 (green), cleaved IL-1 $\beta$  (pink), IL-18 (brown), and DAPI (blue) were stained (D) and counted using ImageJ software in random 10 (resolution: 20-micron) visual fields per each patient. The number of CD68 $^{+}$  particles (E) and CD8 $^{+}$  particles (F) derived from each representative patient with different extents of hepatic inflammation were compared. Then, the data derived from 3 patients with severe hepatitis B was pooled to analyze the correlation between CD68 $^{+}$  cells and effector cytokines (IL-1 $\beta$  $^{+}$  particles and IL-18 $^{+}$  particles) (C), the correlation between CD8 $^{+}$  particles and CD68 $^{+}$  particles (H) and IL-1 $\beta$  $^{+}$  particles (I) with GraphPad Prism 8.0.

(G) Heatmap of Xcell-analyzing data shows intrahepatic immune cell infiltration in patients with different extents of hepatic inflammation as shown in Table 4. Each panel indicates an individual with/without HBV infection. HC, healthy control. \*p < 0.05 and \*\*p < 0.01.

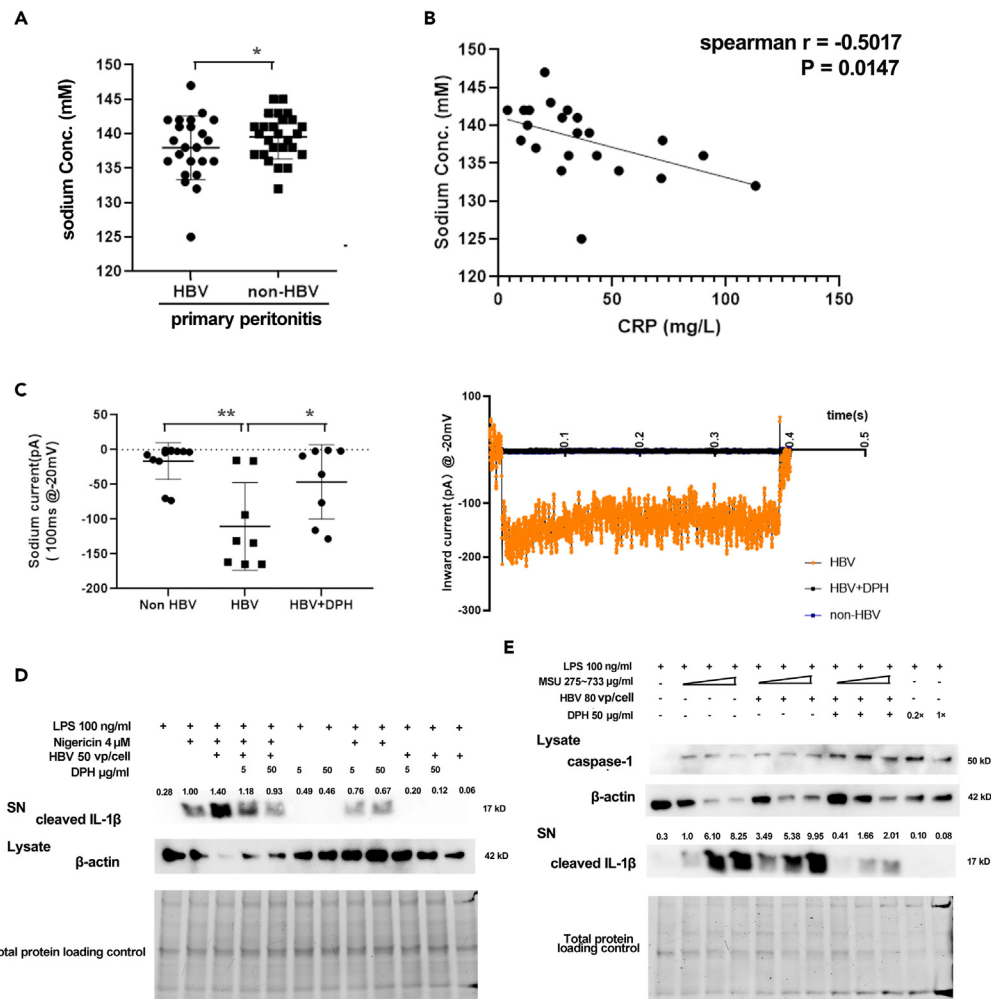


**Figure 7. HBV exposure enhanced NLRP3 activation via increasing sodium influx in macrophages**

(A) Serum sodium concentration was compared between patients with HBV- and non-HBV-related cirrhosis with primary peritonitis.

(B) The correlation between sodium concentration and CRP level was analyzed in HBV-related cirrhosis patients with primary peritonitis.

(C) Sodium influx was assayed by whole-cell patch clamp in THP-1 macrophages exposed or not to HBV, or exposed to HBV plus DPH. Representative currents are shown on the right hand.

(D and E) NLRP3 inflammasome in THP-1 macrophages triggered by nigericin (D) and MSU (E) in combination with DPH and/or HBV were assayed by western blotting. Representative data were shown from one of three independent experiments. \* $p < 0.05$  and \*\* $p < 0.01$ .

In summary, our data suggest NLRP3 inflammasome can be highly activated in HBV-containing context and contributes to HBV-related hepatic inflammation and injury. The synergism of HBV with intrahepatic potential danger signal on potassium efflux promotes activation of NLRP3 inflammasome, which owes to HBV increasing sodium influx in macrophages.

### Limitations of the study

Our data suggest hyperactivation of NLRP3 inflammasome mediated by synergistic effect between HBV and intrahepatic danger signals contributes to hepatic inflammation during HBV infection. But the direct evidence is difficult to obtain, due to lack of a naturally infected mouse model to mimic the natural pathogenesis of HBV infection. Future studies using some clinical data will help to demonstrate this immunopathological mechanism further.

### STAR★METHODS

Detailed methods are provided in the online version of this paper and include the following:

- KEY RESOURCES TABLE
- RESOURCE AVAILABILITY

- Lead contact
- Materials availability
- Data and code availability
- **EXPERIMENTAL MODEL AND STUDY PARTICIPANT DETAILS**
  - Patients with different grades of HBV-associated hepatic inflammation
  - MSU-induced peritonitis model in HBV-tg mouse
  - Cell lines
- **METHOD DETAIL**
  - Investigation of activation and assembly of NLRP3 inflammasome in patients with hepatitis B
  - Investigation of role of activated NLRP3 inflammasome in patients with severe hepatitis B
  - Investigation of HBV-mediated synergistic effect on activation of NLRP3 inflammasome induced by representative potassium-efflux triggers in cell models and HBV-tg models
  - Investigation of mechanism of HBV-mediated synergism on activation of NLRP3 inflammasome in cell models
- **QUANTIFICATION AND STATISTICAL ANALYSIS**

## SUPPLEMENTAL INFORMATION

Supplemental information can be found online at <https://doi.org/10.1016/j.isci.2023.108723>.

## ACKNOWLEDGMENTS

This work was funded by the National Key R&D Program of China (2016YFA0502200), the National Natural Science Foundation of China (Grant No. 31670899 and 32270987) and the Natural Science Foundation of Chongqing (Grant No. CSTC, 2021jcyj-msxmX0657), and Medical Scientific Research major project (Joint Project of Chongqing Health Commission and Science and Technology Bureau) (Grant No. 2019ZDXM004).

## AUTHOR CONTRIBUTIONS

Conceptualization, J.W., X.X., G.H., Y.W.; methodology, J.W., Y.Z., C.C., P.C., J.Z.; investigation, J.W., Q.L., Y.Z., C.C., G.M.; writing – original draft, J.W.; writing – review and editing, J.W., X.X., G.H., Y.W.; supervision, Y.W.; funding acquisition, J.W., X.X., J.Z., Y.W.

## DECLARATION OF INTERESTS

The authors declare no competing interests.

Received: August 3, 2023

Revised: October 3, 2023

Accepted: December 11, 2023

Published: December 21, 2023

## REFERENCES

1. de Carvalho Ribeiro, M., and Szabo, G. (2022). Role of the Inflammasome in Liver Disease. *Annu. Rev. Pathol.* 17, 345–365.
2. Iannacone, M., and Guidotti, L.G. (2022). Immunobiology and pathogenesis of hepatitis B virus infection. *Nat. Rev. Immunol.* 22, 19–32.
3. Sharma, D., and Kanneganti, T.D. (2016). The cell biology of inflammasomes: Mechanisms of inflammasome activation and regulation. *J. Cell Biol.* 213, 617–629.
4. Negash, A.A., Ramos, H.J., Crochet, N., Lau, D.T.Y., Doehle, B., Papic, N., Delker, D.A., Jo, J., Bertoletti, A., Hagedorn, C.H., and Gale, M., Jr. (2013). IL-1 $\beta$  production through the NLRP3 inflammasome by hepatic macrophages links hepatitis C virus infection with liver inflammation and disease. *PLoS Pathog.* 9, e1003330.
5. Li, Y., Yu, P., Kessler, A.L., Shu, J., Liu, X., Liang, Z., Liu, J., Li, Y., Li, P., Wang, L., et al. (2022). Hepatitis E virus infection activates NOD-like receptor family pyrin domain-containing 3 inflammasome antagonizing interferon response but therapeutically targetable. *Hepatology* 75, 196–212.
6. Schroder, K., and Tschopp, J. (2010). The inflammasomes. *Cell* 140, 821–832.
7. Serti, E., Werner, J.M., Chattergoon, M., Cox, A.L., Lohmann, V., and Rehermann, B. (2014). Monocytes activate natural killer cells via inflammasome-induced interleukin 18 in response to hepatitis C virus replication. *Gastroenterology* 147, 209–220.e3.
8. Gaul, S., Leszczynska, A., Alegre, F., Kaufmann, B., Johnson, C.D., Adams, L.A., Wree, A., Damm, G., Seehofer, D., Calvente, C.J., et al. (2021). Hepatocyte pyroptosis and release of inflammasome particles induce stellate cell activation and liver fibrosis. *J. Hepatol.* 74, 156–167.
9. Yu, X., Lan, P., Hou, X., Han, Q., Lu, N., Li, T., Jiao, C., Zhang, J., Zhang, C., and Tian, Z. (2017). HBV inhibits LPS-induced NLRP3 inflammasome activation and IL-1 $\beta$  production via suppressing the NF- $\kappa$ B pathway and ROS production. *J. Hepatol.* 66, 693–702.
10. Faure-Dupuy, S., Delphin, M., Aillot, L., Dimier, L., Lebossé, F., Fresquet, J., Parent, R., Matter, M.S., Rivoire, M., Bendriss-Vermare, N., et al. (2019). Hepatitis B virus-induced modulation of liver macrophage function promotes hepatocyte infection. *J. Hepatol.* 71, 1086–1098.
11. Han, C.Y., Rho, H.S., Kim, A., Kim, T.H., Jang, K., Jun, D.W., Kim, J.W., Kim, B., and Kim, S.G. (2018). FXR Inhibits Endoplasmic Reticulum Stress-Induced NLRP3 Inflammasome in Hepatocytes and Ameliorates Liver Injury. *Cell Rep.* 24, 2985–2999.
12. Molyvdas, A., Georgopoulou, U., Lazaridis, N., Hytiroglou, P., Dimitriadis, A., Foka, P., Vassiliadis, T., Loli, G., Philippidis, A., Zebekakis, P., et al. (2018). The role of the NLRP3 inflammasome and the activation of IL-1 $\beta$  in the pathogenesis of chronic viral hepatic inflammation. *Cytokine* 110, 389–396.
13. Rehermann, B. (2013). Pathogenesis of chronic viral hepatitis: differential roles of T cells and NK cells. *Nat. Med.* 19, 859–868.

14. Kim, J.H., Han, J.W., Choi, Y.J., Rha, M.S., Koh, J.Y., Kim, K.H., Kim, C.G., Lee, Y.J., Kim, A.R., Park, J., et al. (2020). Functions of human liver CD69(+)/CD103(-)CD8(+) T cells depend on HIF-2 $\alpha$  activity in healthy and pathologic livers. *J. Hepatol.* **72**, 1170–1181.
15. Maini, M.K., Boni, C., Lee, C.K., Larrubia, J.R., Reignat, S., Ogg, G.S., King, A.S., Herberg, J., Gilson, R., Alisa, A., et al. (2000). The role of virus-specific CD8(+) cells in liver damage and viral control during persistent hepatitis B virus infection. *J. Exp. Med.* **191**, 1269–1280.
16. Lang, K.S., Georgiev, P., Recher, M., Navarini, A.A., Berghaler, A., Heikenwalder, M., Harris, N.L., Junt, T., Odermatt, B., Clavien, P.A., et al. (2006). Immunoprivileged status of the liver is controlled by Toll-like receptor 3 signaling. *J. Clin. Invest.* **116**, 2456–2463.
17. Ma, Z., Liu, J., Wu, W., Zhang, E., Zhang, X., Li, Q., Zelinsky, G., Buer, J., Dittmer, U., Kirschning, C.J., and Lu, M. (2017). The IL-1R/TLR signaling pathway is essential for efficient CD8(+) T-cell responses against hepatitis B virus in the hydrodynamic injection mouse model. *Cell. Mol. Immunol.* **14**, 997–1008.
18. Kim, T.S., and Shin, E.C. (2019). The activation of bystander CD8(+) T cells and their roles in viral infection. *Exp. Mol. Med.* **51**, 1–9.
19. Nahon, P., Lescat, M., Layese, R., Bourcier, V., Talmat, N., Allam, S., Marcellin, P., Guyader, D., Pol, S., Larrey, D., et al. (2017). Bacterial infection in compensated viral cirrhosis impairs 5-year survival (ANRS CO12 CirVir prospective cohort). *Gut* **66**, 330–341.
20. Xu, P., Han, X., Shen, S., and Li, M. (2021). The Relationship between Serum Uric Acid Level and Liver Function in Patients with Hepatitis B in China. *Clin. Lab.* **67**.
21. Wong, W.M., Wu, P.C., Yuen, M.F., Cheng, C.C., Yew, W.W., Wong, P.C., Tam, C.M., Leung, C.C., and Lai, C.L. (2000). Antituberculosis drug-related liver dysfunction in chronic hepatitis B infection. *Hepatology* **31**, 201–206.
22. Li, P., Kurata, Y., Taufiq, F., Kuwabara, M., Ninomiya, H., Higaki, K., Tsuneto, M., Shirayoshi, Y., Lanaspá, M.A., and Hisatome, I. (2022). Kv1.5 channel mediates monosodium urate-induced activation of NLRP3 inflammasome in macrophages and arrhythmogenic effects of urate on cardiomyocytes. *Mol. Biol. Rep.* **49**, 5939–5952.
23. Schorn, C., Frey, B., Lauber, K., Janko, C., Stryio, M., Keppeler, H., Gaipl, U.S., Voll, R.E., Springer, E., Munoz, L.E., et al. (2011). Sodium overload and water influx activate the NALP3 inflammasome. *J. Biol. Chem.* **286**, 35–41.
24. Muñoz-Planillo, R., Kuffa, P., Martínez-Colón, G., Smith, B.L., Rajendiran, T.M., and Núñez, G. (2013). K<sup>+</sup> efflux is the common trigger of NLRP3 inflammasome activation by bacterial toxins and particulate matter. *Immunity* **38**, 1142–1153.
25. Guo, H., and Ting, J.P.Y. (2020). Inflammasome Assays In Vitro and in Mouse Models. *Curr. Protoc. Immunol.* **131**, e107.
26. Fowler, B.J., Gelfand, B.D., Kim, Y., Kerur, N., Tarallo, V., Hirano, Y., Amarnath, S., Fowler, D.H., Radwan, M., Young, M.T., et al. (2014). Nucleoside reverse transcriptase inhibitors possess intrinsic anti-inflammatory activity. *Science (New York, N.Y.)* **346**, 1000–1003.
27. Ridker, P.M. (2019). Anticytokine Agents: Targeting Interleukin Signaling Pathways for the Treatment of Atherothrombosis. *Circ. Res.* **124**, 437–450.
28. Zanetto, A., Pelizzaro, F., Campello, E., Bulato, C., Balcar, L., Gu, W., Gavasso, S., Saggiolato, G., Zeuzem, S., Russo, F.P., et al. (2023). Severity of systemic inflammation is the main predictor of ACLF and bleeding in individuals with acutely decompensated cirrhosis. *J. Hepatol.* **78**, 301–311.
29. Colloredo, G., Bellati, G., Sonzogni, A., Zavaglia, C., Fracassetti, O., Leandro, G., Ghislandi, R., Minola, E., and Ideo, G. (1999). Semiquantitative assessment of IgM antibody to hepatitis B core antigen and prediction of the severity of chronic hepatitis B. *J. Viral Hepat.* **6**, 429–434.
30. Zhou, J., Song, L., Zhao, H., Yan, L., Ma, A., Xie, S., Zhang, X., Zhang, D., Xie, Q., Zhang, G., et al. (2017). Serum hepatitis B core antibody as a biomarker of hepatic inflammation in chronic hepatitis B patients with normal alanine aminotransferase. *Sci. Rep.* **7**, 2747.
31. Ghany, M.G., Feld, J.J., Chang, K.M., Chan, H.L.Y., Lok, A.S.F., Visvanathan, K., and Janssen, H.L.A. (2020). Serum alanine aminotransferase flares in chronic hepatitis B infection: the good and the bad. *The Lancet. Gastroenterol. Hepatol.* **5**, 406–417.
32. Ben-Sasson, S.Z., Hogg, A., Hu-Li, J., Wingfield, P., Chen, X., Crank, M., Caucheteux, S., Ratner-Hurevich, M., Berzofsky, J.A., Nir-Paz, R., and Paul, W.E. (2013). IL-1 enhances expansion, effector function, tissue localization, and memory response of antigen-specific CD8 T cells. *J. Exp. Med.* **210**, 491–502.
33. Black, J.A., and Waxman, S.G. (2013). Noncanonical roles of voltage-gated sodium channels. *Neuron* **80**, 280–291.
34. Carrithers, M.D., Dib-Hajj, S., Carrithers, L.M., Tokmouline, G., Pypaert, M., Jonas, E.A., and Waxman, S.G. (2007). Expression of the voltage-gated sodium channel Nav1.5 in the macrophage late endosome regulates endosomal acidification. *J. Immunol.* **178**, 7822–7832.
35. Leo, M., Argalski, S., Schäfers, M., and Hagenacker, T. (2015). Modulation of Voltage-Gated Sodium Channels by Activation of Tumor Necrosis Factor Receptor-1 and Receptor-2 in Small DRG Neurons of Rats. *Mediators Inflamm.* **2015**, 124942.
36. Groß, C.J., Mishra, R., Schneider, K.S., Médard, G., Wettmarshausen, J., Dittlein, D.C., Shi, H., Gorka, O., Koenig, P.A., Fromm, S., et al. (2016). K(+) Efflux-Independent NLRP3 Inflammasome Activation by Small Molecules Targeting Mitochondria. *Immunity* **45**, 761–773.
37. Huang, H., Chen, M., Liu, F., Wu, H., Wang, J., Chen, J., Liu, M., and Li, X. (2019). N-acetylcysteine therapeutically protects against pulmonary fibrosis in a mouse model of silicosis. *Biosci. Rep.* **39**, BSR20190681.
38. Jobin, K., Müller, D.N., Jantsch, J., and Kurts, C. (2021). Sodium and its manifold impact on our immune system. *Trends Immunol.* **42**, 469–479.
39. Biggins, S.W., Kim, W.R., Terrault, N.A., Saab, S., Balan, V., Schiano, T., Benson, J., Therneau, T., Kremers, W., Wiesner, R., et al. (2006). Evidence-based incorporation of serum sodium concentration into MELD. *Gastroenterology* **130**, 1652–1660.
40. Heymann, F., and Tacke, F. (2016). Immunology in the liver—from homeostasis to disease. *Nat. Rev. Gastroenterol. Hepatol.* **13**, 88–110.
41. Chinese Society of Infectious Diseases, Chinese Medical Association, Chinese Society of Hepatology, Chinese Medical Association (2019). The guidelines of prevention and treatment for chronic hepatitis B (2019 version). *Chin. J. hepatol.* **27**, 938–961.
42. Guido, M., Mangia, A., and Faa, G.; Gruppo Italiano Patologi Apparato Digerente GIPAD, Società Italiana di Anatomia Patologica e Citopatologia Diagnostica/International Academy of Pathology, Italian division SIAPEC/IAP (2011). Chronic viral hepatitis: the histology report. *Dig. Liver Dis.* **43**, S331–S343.

**STAR★METHODS**

**KEY RESOURCES TABLE**

REAGENT or RESOURCE	SOURCE	IDENTIFIER
<b>Antibodies</b>		
anti-Caspase-1 p10	Santa	sc515 RRID:AB_630975
anti-Caspase-1 p20	Cell signaling Techonology	2225
anti-caspase-1	AdipoGen	AG-20B-0042 RRID:AB_2490248
anti-P2X7	Abcam	ab109246 RRID:AB_10858498
anti-NLRP3	Santa	sc134306 RRID:AB_2152550
anti-NLRP3	Sigma-Aldrich	HPA012878 RRID:AB_1846752
anti-cleaved IL-1 $\beta$	Cell signaling Techonology	83186
anti-IL-1 $\beta$	Cell signaling Techonology	12426
anti- IL-1 $\beta$	R&D	AF-401-NA RRID:AB_416684
anti-IL-18	Abcam	ab243091 RRID:AB_2861283
anti-cleaved GSDMD c terminal	Cell signaling Techonology	36425s
Hepatocyte antigen 1	Abcam	ab129076 RRID:AB_11156290
anti-P2X7	Cell signaling Techonology	13809
anti- $\beta$ actin	Cell signaling Techonology	3700
anti-Nav1.5	Proteintech	23016-1-AP RRID:AB_2879198
anti-Nav1.6	Abcam	ab65166 RRID:AB_1143010
anti-Nav1.7	FineTest	FNab07646
anti-CD11b PE-cy7	eBioscience	25-0112-82
anti-Ly6C FITC	BioLegend	128005 RRID:AB_1186134
anti-Ly6G PE	BioLegend	127607 RRID:AB_1186104
anti-CD68	Immunoway	YM3050 RRID:AB_2923241
anti-CD8	Affinity	AF5126 RRID:AB_2837612
Donkey polyclonal anti-rabbit Ig(H+L) Alexa Fluor 555 conjugated	Invitrogen	A31572
Donkey polyclonal anti-mouse Ig(H+L) Alexa Fluor 488 conjugated	Invitrogen	A21202
<b>Chemicals</b>		
A438079	MCE	HY-15488
A740003	MCE	HY-50697
Suramin	MCE	HY-B0879A
uric acid	Sigma-Aldrich	U2875

(Continued on next page)

**Continued**

REAGENT or RESOURCE	SOURCE	IDENTIFIER
uric acid crystal	InvivoGen	tlrl-msu
Nigericin	MCE	HY-100381
LPS	Sigma-Aldrich	L2654
Phenytoin sodium (DPH)	MCE	HY-B0448A
ATP	InvivoGen	tlr1-atp
BzATP	MCE	HY-13954
oATP	Sigma-Aldrich	5057580001
NAC	MCE	HY-134495
Imiquimod	MCE	HY-B0180
entecavir	MCE	HY-13623
Dynabeads protein G	Dynal	10003D
PMA	MCE	HY-18739
Normocin	InvivoGen	ant-nr-2
M-CSF	Peptotech	Cat #315-02
<b>Critical Commercial Assays</b>		
Mycoplasma detection kit	InvivoGen	rep-mys-10
Caspase-1 activity assay kit	BioVision	K111
ATP assay kit	Sigma-Aldrich	FLAA-1KT
Caspase-1 p20 assay kit	R&D	DCA100
Human IL-1 $\beta$ ELISA assay kit	ThermoFisher	BMS224-2
Human IL-1 $\beta$ ELISA assay kit	Invitrogen	88-7261-88
Mouse IL-1 $\beta$ ELISA assay kit	Invitrogen	88-7013-88
Human IL-18 ELISA assay kit	Raybiotech	ELH-IL18
M30 assay kit	Peviva	M30-Apoptosense
chemiluminescence reagents	Millipore	34095
BS3 cross-linker agent	ThermoFisher Scientific	A39266
<b>Animal, cell line</b>		
HBV-tg mouse (genotype A)	Weitongda Inc.	B6-Tg (HBV)5 Vst /Vst
THP-1 cell lines	ATCC	TIB-202
HepG2 cell line	Procell	CL-0103
C57/BL	GemPharmatech	N/A
<b>Nucleic acid and sequencing data</b>		
HBV1.3 plasmid (genotype D, Accession:HE974378)	This paper	N/A
LV-puro-NTCP	Tsingke Technology	N/A
RNA sequencing data	Biomarker	HRA005989
<b>primer for HBV quantification</b>		
HBV1844 F : 5'-GTTGCCCGTTTGTCTCTAATTC-3'		This paper
HBV1745 R: 5'-GGAGGGATACATAGAGGTTCTTGA-3		
<b>Software</b>		
Prism 8.0	GraphPad Software	N/A
Image J	NIH	N/A
Image Lab	BioRad	N/A
Flowjo	BD	N/A
Clampfit	Molecular Devices	N/A

## RESOURCE AVAILABILITY

### Lead contact

Further information and requests for resources and reagents should be directed to and will be fulfilled by the lead contact, Jingxue Wang [jingxue.wang@hotmail.com](mailto:jingxue.wang@hotmail.com).

### Materials availability

This study did not generate new unique reagents.

### Data and code availability

- Data: RNA Sequencing data have been deposited at the Genome Sequence Archive of National Genomics Data Center (Accession number: GSA-Human: HRA005989), and are publicly available as of the date of publication.
- Code: This study does not report any original code.
- Any additional information required to reanalyze the data reported in this paper is available from the [lead contact](#) upon request.

## EXPERIMENTAL MODEL AND STUDY PARTICIPANT DETAILS

### Patients with different grades of HBV-associated hepatic inflammation

Four different patient cohorts with HBV infection were analysed. The first group was clinically relevant data of patients with cirrhosis with primary peritonitis, including HBV and non-HBV infection. The second and third groups were plasma samples, and the fourth group was liver biopsy samples. All samples and data were collected at the First Affiliated Hospital of Chongqing Medical University from 2019 to 2021, and the study was approved by the ethics committee of the First Affiliated Hospital of Chongqing Medical University (Study ID:2019-266, 16/10/19). Baseline characteristics of patients were presented in Tab. 1–4. Written informed consent was obtained from patients. Liver tissues from the eight liver transplant donors were used as healthy controls.

CHB was diagnosed according to the Guidelines of prevention and treatment for chronic hepatitis B.<sup>41</sup> The active hepatitis phase in HBV-infected patients was identified according to ALT >40 IU/mL or modified histological activity index (HAI) ≥ 6. Inflammatory activity was graded using a modified HAI<sup>42</sup> in liver biopsy specimens and/or clinical characteristics in plasma specimens (if modified HAI was not available); inflammatory activity was classified as minimal hepatic inflammation (modified HAI < 6, ALT < 40 IU/mL and TBIL < 25 μM) or severe hepatitis. Severe hepatitis was identified by modified HAI ≥ 6 or either of the following three condition: an abrupt elevation in serum ALT ≥ 200 IU/mL; TBIL ≥ 100 μM; prothrombin time international normalized ratio (PT INR) ≥ 1.2 as described previously.<sup>28–30</sup> The fibrosis stage was evaluated according to the METAVIR score.

### MSU-induced peritonitis model in HBV-tg mouse

The HBV-transgenic (tg) Mice (C57BL/6 strain, male, 6–8 week) were purchased (Weitongda, Beijing) and maintained under P2 conditions. All experimental animal procedures were approved by the Laboratory Animal Welfare and Ethics Committee of the Army Medical University (AMUWE2019393). The HBV-tg mouse and 6–8 week old male C57BL/6 mice were used to build peritonitis model. In brief, MSU crystal (0.75 mg/each mouse suspended in 150 μl sterile PBS) was injected into peritoneal cavity of mouse using 1 ml insulin syringe. Then, collected the peritoneal lavage carefully 6 h later avoiding blood contamination and harvested the cells infiltrated from peritoneal lavage to perform FACS assay.

### Cell lines

#### THP-1

The THP-1 cell lines were differentiated by 100 ng/ml PMA for 24h, and then rest for 24h to be used for inflammasome activity assay. The medium for THP-1 cell lines is RPMI 1640 containing 10% fetal bovine serum (Gibco Laboratories, Grand Island, NY), 100 IU/ml of penicillin, 100 μg/ml streptomycin, 2 mM L-glutamine and 0.1mg/ml Normocin.

#### Bone marrow-derived macrophages (BMDMs)

The BMDMs were extracted from leg bones and induced by macrophage colony-stimulating factor (M-CSF, 200 μg/ml) in DMEM containing 10% fetal bovine serum (Gibco Laboratories, Grand Island, NY), 100 IU/mL of penicillin, 100 μg/ml streptomycin, 2 mM L-glutamine and 0.1mg/ml normocin for 5 days. The M-CSF was supplemented in half every 2 days.

#### Peripheral blood mononuclear cell (PBMC)

Human PBMCs are isolated from peripheral blood through density gradient centrifugation. In brief, diluted the whole blood at 1:1 volume ratio and added gently over the density gradient medium (Lymphoprep, STEM CELL). After centrifugation with 400g for 20min, harvested the mononuclear cells and washed twice with PBS. Then these cells were cultured for 12–24h. The stimulatory experiments were performed in the second day.

### HepG2-NTCP

The HepG2 were cultured in DMEM containing 10% fetal bovine serum (Gibco Laboratories, Grand Island, NY), 100 IU/ml of penicillin, 100 µg/ml streptomycin, 2 mM L-glutamine and 0.1 mg/ml Normocin. HepG2 were seeded at a cell density of  $0.5 \times 10^5$  cells/cm<sup>2</sup> in 2 ml of medium. After 12h, cells were transfected with lentivirus containing NTCP coding sequence at a multiplicity of infection of 30. The HepG2-NTCP cell lines would be selected by puromycin for 2 weeks, and then were infected by HBV.

## METHOD DETAIL

### Investigation of activation and assembly of NLRP3 inflammasome in patients with hepatitis B

#### *Treatment of samples (plasma and liver tissue) derived from patients*

Some liver biopsy samples were grind and incubated in RIPA buffer for 15-30 min on ice, and then used for western blot and co-immunoprecipitation (Co-IP) assay. Some liver biopsy samples were grind and incubated in lysis buffer provided by manufacture for 15-30 min on ice, and then used for caspase-1 p20 activity assay (BioVision, CA, USA). Some liver biopsy was immediately fixed in 4% paraformaldehyde for 24h immediately after saline irrigation, and then embedded with paraffin for subsequent immunofluorescence histochemistry and multiplex immunofluorescence staining. Additionally, some liver biopsy samples were stored in Allprotect Tissue Reagent (Qiagen, Hilden, Germany) at -80°C for subsequent purification of RNA isolation and transcriptome sequencing.

Plasma samples were separated from the patients' whole blood samples (in Sodium citrate tubes) by centrifugation and stored at -80°C in aliquots appropriate for individual use in subsequent ELISA assay for IL-1β, IL-18 and caspase-1 p20 subunits.

#### *Measurement of cytokines and caspase-1 p20 subunits in patients' plasma*

Activation of inflammasome in macrophages would release IL-1β, IL-18 and caspase-1 p20, and increased IL-1β, IL-18 and caspase-1 p20 subunits in patients' plasma can be investigated with ELISA. The cytokine IL-1β in patients' plasma was assayed with Human IL-1β ELISA assay kit (BMS224-2, ThermoFisher), according to manufacturer's advices. The cytokine IL-18 and caspase-1 p20 subunits were also assayed with ELISA Kit (shown in [key resources table](#)).

#### *Measurement of NLRP3 inflammasome activation and assembly in patients' liver tissues*

**Assays for intrahepatic activation of NLRP3 inflammasome.** The liver tissues were grind and incubated in RIPA buffer for 15-30 min on ice, and then used for western blot. The liver tissue protein (20-60 µg) was run on a 12% sodium dodecyl sulphate-polyacrylamide gel (SDS-PAGE gel), and electro-transferred to a polyvinylidene fluoride membrane. The membranes were then probed with primary antibodies (anti-caspase-1 p20) overnight at 4°C, and subsequently incubated with secondary antibody for 45min. Immuno-detection was performed using chemiluminescence reagent. Quantitative analysis was performed using optical (grayscale) density (ImageJ software, normalised by β-actin).

Liver tissue lysates (100 µg) from patients with chronic hepatitis B and normal donors were assayed for caspase-1 activity, according to the caspase-1 colorimetric assay kit manufacturer's instructions (K111-100, BioVision, USA).

The total RNAs were extracted from 6 liver samples from normal donor, minimal and severe HBV-related hepatic inflammation patients and submitted to RNA Sequencing (BIOMARKER Technology). The library was constructed following Illumina's TruSeq Stranded mRNA sample preparation protocol, and library concentration and insert size was checked with Qubit2.0 and Agilent 2100. After passing library quality inspection, Illumina platform was used to carry out high-throughput sequencing. HISAT2 (<http://daehwankimlab.github.io/hisat2/>) was used to map reads to the genome, and StringTie (<https://ccb.jhu.edu/software/stringtie/>) was used to assemble the transcripts with mapped reads. The raw sequence data reported in this paper have been deposited in the Genome Sequence Archive of National Genomics Data Center, China National Center for Bioinformatics / Beijing Institute of Genomics, Chinese Academy of Sciences (GSA-Human: HRA005989) that are publicly accessible at <https://ngdc.cncb.ac.cn/gsa-human>.

DESeq2 is used for identifying differentially expressed genes of 3 group transcripts. During identifying differentially expressed genes, Fold Change (FC) ≥ 1.5 and P value < 0.01 were used as the screening criteria. DEGs were subjected for KEGG pathway enrichment analysis in R (version 4.1.0).

**Assays for intrahepatic assembly of NLRP3 inflammasome.** For investigation on assembly of NLRP3 inflammasome in liver tissues, anti-NLRP3 and anti-P2X7 antibodies were cross-linked with Dynabeads Protein G using the BS3 cross-linker agent in a conjugation buffer (100 mM sodium phosphate, 0.15 M NaCl, 20 mM HEPES, 100 mM bicarbonate) for 30 min at room temperature (20°C), according to manufacturer's instructions. Then the beads were added into 100 µg liver tissue proteins and incubated for 2h at 4°C with rotation. The protein captured with anti-NLRP3 and anti-P2X7 was eluted with 50mM Glycine (PH2.8), loaded on 12% SDS-PAGE gel and then electro-transferred to a polyvinylidene fluoride membrane. The membrane was probed with anti-caspase-1 antibody. Thus, caspase-1 protein bound with NLRP3 or P2X7 was measured and compared in patients with severe hepatitis B and healthy control using optical (grayscale) density (ImageJ software, normalised by β-actin).

We also explore another way to investigate assembly of NLRP3 inflammasome through co-localization of NLRP3 inflammasome components. After heat-induced epitope retrieval in 10 mM sodium citrate (pH 6.0) for 8min, paraffin-embedded sections were incubated in 3% H<sub>2</sub>O<sub>2</sub> and blocked in 3% goat or rabbit serum buffer. Sections were incubated with goat or rabbit-derived primary antibodies overnight at 4°C. Then fluorescence-labeled donkey anti-Goat or donkey anti-rabbit secondary antibody were used to visualize the staining. The

sections were assessed and imaged on an epifluorescence imaging microscope (B51; Olympus, Tokyo, Japan). Confocal images were obtained using LSM780NLO multiphoton microscope (Zeiss, Oberkochen, Germany).

### **Investigation of role of activated NLRP3 inflammasome in patients with severe hepatitis B**

#### *Assessment of association between inflammasome activation and intrahepatic numbers of infiltrated CD8<sup>+</sup> and CD68<sup>+</sup> cells*

We first explore a sequential multiplex immunofluorescence to assessment numbers of intrahepatic inflammatory infiltrates. For sequential multiplex immunofluorescence staining on the same paraffin-embedded liver slide, two different combinations of antibodies for assay were used: CD68, Hepatocyte antigen 1, CASP1, c-GSDMD and DAPI as well as CD68, CD8, cleaved IL-1 $\beta$ , IL-18 and DAPI. Images were acquired using Panoramic SCAN II (3DHISTECH, Hungary). On the same slide, CD68 (red), CD8 (green), cleaved IL-1 $\beta$  (pink), IL-18 (brown) and DAPI (blue) were stained and counted using ImageJ software in random 10 (resolution: 20-micron) visual fields per each patient. The analysis of number of CD68<sup>+</sup> and CD8<sup>+</sup> particles derived from each representative patient with different extents of hepatic inflammation suggested increased intrahepatic infiltration with the extent of inflammation. Then, the data derived from 3 patients with severe hepatitis B was pooled to analyse the correlation between CD68<sup>+</sup> cells and effector cytokines (IL-1 $\beta$ <sup>+</sup> particles and IL-18<sup>+</sup> particles), the correlation between CD8<sup>+</sup> particles and CD68<sup>+</sup> particles and IL-1 $\beta$ <sup>+</sup> particles. These data implied IL-1 $\beta$ , which is majorly derived from CD68<sup>+</sup> cells, contributed in an increase of intrahepatic CD8<sup>+</sup> T cells.

Secondly, we explore X cell-analysing to show an increased intrahepatic immune cell infiltration in patients with different extents of hepatic inflammation, based on transcriptome sequencing data.

#### *Association analysis between NLRP3 inflammasome effector and hepatic injury markers in plasma*

ELISA was carried out using commercially available assay kits for M30 (M30-Apoptosense; Peviva, Sweden). Absorbance was read using an iMark microplate reader (Bio-Rad, USA). The correlation between effector cytokines (IL-1 $\beta$  and IL-18) and hepatic injury markers (ALT and M30) in plasma of patients' with severe hepatitis B was analyzed using Spearman's rank correlation test.

### **Investigation of HBV-mediated synergistic effect on activation of NLRP3 inflammasome induced by representative potassium-efflux triggers in cell models and HBV-tg models**

#### *Macrophage culture and stimulation*

The macrophage was primed with LPS 100-1000 ng/ml for 3-6 h, and then stimulated with ATP 5 mM, or Nigericin 20  $\mu$ M, or MSU crystal 100-1000  $\mu$ g/ml for 0.5-6 h. The HBV was added in the medium at the same time with ATP, or Nigericin, or MSU. We used potassium chloride to raise the extracellular potassium ion concentration and block the intracellular potassium ion efflux, thereby inhibiting the activation of NLRP3 inflammasome induced by potassium efflux signaling. The cytokine IL-1 $\beta$  in cultured cells including THP-1 macrophages and PBMC was assayed with Human IL-1 $\beta$  ELISA assay kit (88-7261-88, Invitrogen). The cytokine IL-1 $\beta$  in BMDM cell medium was assayed with Mouse IL-1 $\beta$  ELISA assay kit (88-7013-88, Invitrogen).

#### *Preparation of HBV particles*

HBV was produced by HepG2 transfected by HBV1.3 plasmids (genotype D, strain ayw, NC\_003977) with Lipofectamine 3000 (Invitrogen). After transfection 3 days, the supernatant was harvested and concentrated by 6% PEG6000 containing 0.5M NaCl. The HBV particles were suspended with PBS and quantified by QPCR. The vehicle control used supernatant derived from HepG2 cell lines transfected by vector plasmid and was prepared with same concentrating protocol at same time.

#### *Western blotting for NLRP3 activation triggered by different signals in combined with HBV treatment*

Whole cell lysates were obtained using RIPA buffer, and the supernatant (SN) (cell culture medium) was concentrated in 15% trichloroacetic acid, and resolved with 10 mM Tris (pH 7.5) containing 500 mM sodium bicarbonate. All samples were electrophoresed on a 12% sodium dodecyl sulphate-polyacrylamide gel or 10-12% TGX Stain-Free gel at 4°C, and electro-transferred to a polyvinylidene fluoride membrane. The membranes were then probed with primary antibodies overnight at 4°C, and subsequently incubated with secondary antibody for 45min. Immuno-detection was performed using enhanced chemiluminescence reagent. Quantitative analysis was performed using optical (grayscale) density (ImageJ software, normalised by  $\beta$ -actin; and Bio-Rad Image Lab software, normalised by total protein loading control).

#### *Flow cytometry analysis of infiltrated inflammatory cells in peritonitis mice*

We compared the inflammatory infiltration in the peritoneal cavity of HBV-tg and wild-type mice, and assessed the effect of HBV exposure on NLRP3 inflammasome-mediated inflammatory response *in vivo*. The HBV-tg mouse and 6-8 week old male C57BL/6 mice were build peritonitis model. Then, harvested the cells infiltrated from peritoneal lavage and add anti-CD16/32 antibody (1:50 in FACS buffer) into cells to block Fc receptors on ice for 10 min, and subsequently add monoclonal antibodies of same volume against mouse CD11b and Ly-6G (BioLegend, San Diego, CA, USA; eBiosciences, San Diego, CA, USA) into cell suspension and incubate on ice for 30 min. Run the samples on the BD FACSCanto II and analyze the ratio of neutrophils (CD11b<sup>+</sup> Ly-6G<sup>+</sup>) using Flowjo software.

### *Clinical data for analysing HBV-associated hepatic inflammation in patients with decompensated cirrhosis and primary peritonitis*

The adenosine triphosphate (ATP) signals are a kind of common intrahepatic danger signals, which activates NLRP3 inflammasome via potassium efflux. Through confocal microscopy and Co-IP as described above, we observed P2X7 receptor was involved in intrahepatic assembly of NLRP3 inflammasome in the liver of patients with severe hepatitis B. And through correlation analysis, we observed both ATP levels and HBV particles were positively associated with caspase-1 p20 levels in plasma of patients with severe hepatitis B. These data implied HBV-mediated synergism with ATP signal enhanced intrahepatic activation of NLRP3 inflammasome in patients with severe hepatitis B.

### **Investigation of mechanism of HBV-mediated synergism on activation of NLRP3 inflammasome in cell models**

#### *Whole-cell patch-clamp assay for HBV-mediated sodium influx in THP-1 macrophages*

For sodium current assay, Thp-1 macrophages were prepared as described, and then transferred into Opti-MEM medium (bath solutions). And Patch pipettes were filled with a solution containing 145 mM KCl, 10 mM EGTA and 10 mM HEPES (pH 7.3). Upon exposure to HBV (100 vp/cell) for 5-10min, patch pipettes were sealed tightly, and whole-cell currents were recorded on an Axopatch 200B amplifier (Axon Instruments, Foster City, CA). The IV-curve for  $I_{Na(V)}$  (voltage-gated sodium channel current, VGSC current) was recorded for depolarizing steps starting at  $-60\text{mV}$  and increased stepwise by  $10\text{mV}$  to maximum depolarization of  $+60\text{mV}$ . Current data were filtered at 1 kHz using a four-pole Bessel filter and digitized at a rate of 10 KHz employing a Digidata 1440B (Axon Instruments). Data were recorded only from cells with access resistance of less than  $15\text{M}\Omega$ , and series resistance was compensated. Thp-1 macrophages were voltage-clamped at  $-70\text{mV}$ . All experiments were performed at room temperature ( $22\text{-}25^\circ\text{C}$ ).

#### *WB assay for blockage of HBV-mediated synergism by non-specific sodium channels inhibitor*

The THP-1 macrophages were primed with LPS 100-1000 ng/ml for 3-6 h, and then stimulated with Nigericin  $4\text{ }\mu\text{M}$  and HBV particles with or without DPH for 0.5h, or MSU crystal 275-733  $\mu\text{g}/\text{mL}$  and HBV with or without DPH for 6 h. The HBV was added in the medium at the same time with Nigericin, or MSU.

### *Clinical data: More severe hyponatremia in patients with HBV-associated cirrhosis with primary peritonitis*

By analysing clinical data from patients with cirrhosis with primary peritonitis, a group of age- and sex-matched patients with cirrhosis and primary peritonitis were collected, and compared their level of sodium and C reactive protein (CRP) in serum between HBV- and non-HBV-infected patients. We observed lower sodium concentrations and higher CRP levels in HBV-infected patients, compared with non-HBV infected patients with cirrhosis with primary peritonitis. And a significant negative association was displayed between sodium concentration and CRP level in 23 patients with HBV-related but not non-HBV-related decompensated cirrhosis and primary peritonitis.

### **QUANTIFICATION AND STATISTICAL ANALYSIS**

All data were analysed using the GraphPad Prism 8.0 software. Multiple comparisons were made between the different groups using one-way analysis of variance and Turkey's multiple comparisons. Comparisons between two independent groups were performed using unpaired two-tailed t-tests. Correlations between variables were evaluated using Spearman's rank correlation test.